Gazelle: Energy-Efficient Wearable Analysis for Running

Qi Liu, *Student Member, IEEE*, James Williamson, *Student Member, IEEE*, Kun Li, Wyatt Mohrman, Qin Lv, Robert P. Dick, *Member, IEEE*, and Li Shang, *Member, IEEE*

Abstract—Running is one of the most popular sports with hundreds of millions of participants worldwide. Good running form is the key to fast, efficient, and injury-free running. Existing kinematic analysis technologies, such as high-speed camera systems, are expensive, difficult to operate, and exclusive to sports physiology laboratories and elite athletes. Miniature MEMS-based motion sensors enable portable high-precision kinematic analysis, but suffer from high energy consumption hence short battery lifetime, especially for continued online analysis for running. This paper presents Gazelle, a wearable online analysis system for running that is compact, lightweight, accurate, and highly energy efficient; intended for runners of all levels. To enable long-term maintenance-free mobile analysis for running, Sparse Adaptive Sensing (SAS) is proposed, which selectively identifies the best sampling points to maintain high accuracy while greatly reducing sensing and analysis energy overheads. Experimental results demonstrate 97.7 percent accuracy with 76.9 to 99 percent reduced energy consumption (83.6 percent average reduction under real-world testing)-a one-order-of-magnitude improvement over existing solutions. SAS enables > 200 days of continuous high-precision operation using only a coin-cell battery. Since 2014, Gazelle has been used by over 100 elite and recreational runners during daily training and at top-level races like the Kona Ironman World Championships and New York Marathon.

Index Terms—Wearable technology, energy-efficient analysis, sparse adaptive sensing, running form analysis

---◆---

1 INTRODUCTION

RUNNING is the number one participatory sport. It is estimated that there are over 200 million regular runners in the world [1], [2]. Runners have a yearly injury rate of 50-70 percent [3]. There is a consensus among physiologists that poor running form has a major impact on injury rates. Analyzing and improving running form can reduce injury rate and can also help runners to improve performance.

Sports physiologists and coaches have studied running form for over a century [4]. Quantitative assessment of running form is mostly constrained to the laboratory environment. Sports physiology labs are commonly equipped with high-speed video cameras. To perform a test, markers are attached to various reference points on the runner's body. Calibration while standing is then performed. The test subject finally runs on a treadmill, while the 3D positional trajectory of each marker is determined over time [5]. This type of analysis has been limited to small-scale research studies and the support of elite athletes, due to the high equipment cost, the need of a special laboratory environment, and the lengthy setup and post processing time. The data collected is of

limited time duration and is collected in a static and controlled environment. Long-term running form effects, such as what occurs over the course of training plans lasting weeks and months, and effects due to a runner's negotiation of natural outdoor terrain and weather are not captured.

Economical MEMS inertial measurement units (IMUs), such as accelerometers and gyroscopes, are widely used in mobile phones and are able to accurately sense motion, tracking the acceleration, velocity, and position of the human body. These technologies enable low-cost wearable kinematic-analysis [6], [7], [8], [9]. When paired with wireless data links, such as Bluetooth Low Energy, IMU sensor platforms enable real-time feedback to the user, allowing runners to learn from the result of form changes in-situ and on-the-fly. However, it is challenging to implement compact, accurate IMU-based kinematic analysis systems for running that both work in realtime and have long battery lifetimes.

Energy efficiency is therefore a foremost concern for wearables as 1) their compact form factors leave little space for large batteries, and 2) users are not accepting of wearable devices needing frequent recharging. Compared with mobile phones, which are typically equipped with batteries storing thousands of mAh of energy, the batteries used in wearables generally only have tens of mAh to a few hundred mAh of energy capacity. In addition, while people typically charge their smart phones everyday, the expected battery lifetime for wearables ranges from weeks to months. For example, running foot pods now in the marketplace (primarily measuring a runner's speed and distance run) are simplistic in operation and work for one year without recharging. Users attach them to the shoe laces, and do not need to worry about

- Q. Liu, J. Williamson, K. Li, W. Mohrman, Q. Lv, and L. Shang are with the Department of Electrical, Computer, and Energy Engineering, University of Colorado, Boulder, CO 80309. E-mail: {qi.liu, james.a.williamson, kun.li, wyatt.mohrman, qin.lv, li.shang}@colorado.edu.
- R.P. Dick is with the Department of Electrical Engineering and Computer Science, University of Michigan, Ann Arbor, MI 48109. E-mail: dickrp@umich.edu.
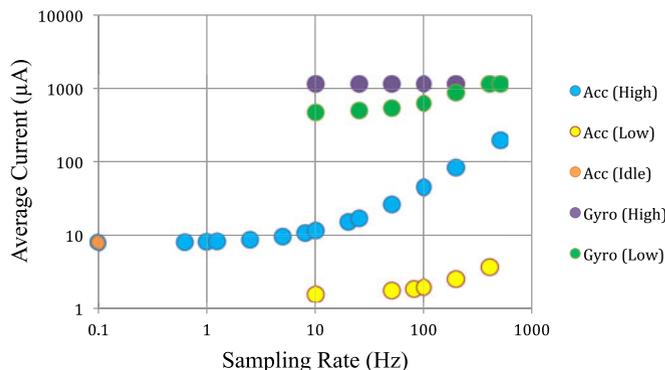
Fig. 1. Power consumption of MEMS IMU sensors: Accelerometer, gyroscope, and low-power accelerometer currents are shown across frequency and operational mode.

them until it is time to replace the shoes themselves. The expectation of users has already been set. The new device we build must adhere to this standard or be rejected by users. Overall, the energy budget for wearables is orders of magnitude smaller than that of mobile phones.

The energy consumption of mainstream economical MEMS IMUs sensors, although appropriate for mobile phones, is not suitable for ultra-compact wearables. Specifically, economical MEMS IMUs sensors have high active and/or idle currents. For instance, mainstream MEMS gyroscopes have active currents in the mA range, which would limit the battery lifetime of a wearable to a few days. More importantly, the power consumption of MEMS IMUs sensors is a function of sampling rate. As shown in Fig. 1, the active current of an accelerometer may increase by over an order of magnitude at high sampling rates. High-precision kinematic analysis potentially requires a high data sampling rate, imposing high computation and energy overheads; this is the primary barrier to wearable devices supporting high-precision running form analysis. There is need for energy-efficient sensing and analysis solutions to accommodate economical MEMS IMUs sensors technologies, yet providing high-precision running form analysis at runtime.

This paper presents *Gazelle*, a wearable kinematic analysis system with the goal of delivering both short and long term quantitative understanding of personal running form to all runners, helping people run faster, longer, and safer. Gazelle is compact in size, lightweight, and equipped with a new sparse adaptive sensing (SAS) algorithm, which utilizes the strengths of a low power and a high power accelerometers, greatly reduces data sensing and analysis overhead, yet maintains high running form analysis accuracy. Gyroscope is not used in the SAS algorithm due to its infeasible long startup time for intra-stride adaptive sensing. We can solve this problem by using inter-stride adaptive sensing for gyroscope and we have achieved significant energy reduction with high running metric accuracy, however, this beyonds the scope of this work and hence is not included in this paper.

The proposed SAS algorithm is motivated by the fact that runners tend to maintain a consistent running form across many strides, so that sparse sensing at lower sampling rates can still capture the targeted running form metrics. Furthermore, the sparse sensing process can be adaptive, i.e., we can vary the data sampling rate within a detected stride by predicting where the critical points exist in time, further

reducing the number of samples needed for accurate analysis. Our experimental study shows that SAS can reduce the data sensing and analysis overhead, hence the energy consumption, by 76.9 percent while maintaining 97.7 percent accuracy. This allows Gazelle to have a small form factor, with a total weight of less than 8 grams, yet offering over 200 days of use on a standard coin-cell battery.

This paper makes the following contributions:

- The design of *Gazelle*, a wearable system that is compact in size, lightweight, and highly energy efficient for long-term, online running form analysis;
- The design of the sparse adaptive sensing algorithm, which exploits the variability of the running signal to sample adaptively in time, thus reducing energy consumption yet still maintaining high accuracy;
- Real-world evaluation using in-lab experiments and pilot studies with runners during day-to-day training and racing, including our study of eight top professional and amateur athletes using Gazelle during the Kona Ironman World Championship race.

The rest of the paper is organized as follows. Section 2 reviews prior work. Section 3 presents an overview of the Gazelle system. Section 4 validates our running form analysis approach as compared with a laboratory kinematic analysis system. Section 5 describes our SAS algorithm. Section 6 presents the experimental results and pilot study results. Finally, Section 7 concludes the work.

2   RELATED WORK

Sports physiologists and coaches have long been studying running form and its impact on running performance and safety. High-speed video camera systems and floor-mounted force plates have been the de-facto equipment in sports physiology laboratories and have effectively supported running kinematic research [5], [10], [11], [12], [13], [14]. The limitations of such systems include high cost, time-consuming operation, and their use is confined to the indoor lab-testing scenario. Major sports brands have also developed pedometer-based wearable solutions to help people run better [15], [16], [17], [18]. Gazelle offers longer battery lifetime with much more detailed and comprehensive running form analysis.

Recently, researchers have been using wearable sensing technologies to facilitate in-lab running kinematic analysis or out-of-lab studies [6], [7], [8], [19], [20], [21], [22]. Several wearable kinematic analysis prototypes have been developed using IMUs. These projects mainly used the wearable devices for data collection for offline analysis. There were few studies investigating the power consumption of an IMU-based kinematic analysis system, which showed limited battery lifetime of only a few days [8]. In the general motion or activity sensing area, there exists a lot of research on the problem of energy management [23]. There are mainly two categories of power saving methods: sensor duty-cycling and collaborative sensing with multiple sensors [24], [25], [26], [27]. For example, in the mobile sensing framework designed by Wang et al. [23], only a minimum set of sensors were powered and appropriate sensor duty cycles were used to significantly improve device battery life. Ganti et al. and Zhu et al. also utilized sensor duty-cycle to minimize power consumption by detecting the active and
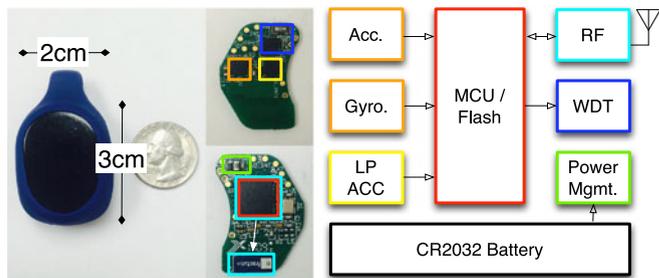
Fig. 2. The Gazelle wearable sensor and system architecture.

idle state of user [28], [29]. In the E-Gesture work done by Park et al., the authors proposed a collaborative sensing technique that used accelerometer and gyroscope based gesture detectors, and the gyroscope detector was only activated when a valid gesture was detected by the accelerometer detector to reduce energy consumption [30]. In our work, besides leveraging those power saving techniques, we also propose a sparse adaptive sensing algorithm with the collaboration of two accelerometers to reduce the sensor power consumption during active mode. Although our method is tuned for online running form analysis, it can also be applied to other sensing fields.

In terms of sparse or adaptive sampling algorithms at signal level, various model-based theoretical analysis has been conducted in signal processing and wireless communication [31], [32], [33], [34], [35]. These work utilized the sparsity of the signal, and the local signal time-frequency variance to minimize sampling overhead. For example, compressed sensing [31], [32], [33] does sparse, random sampling based on the sparsity of a signal in a sparse domain (e.g., frequency domain) though the signal may not be sparse in the time domain. As a result, though these work were used in wearable sensing devices, only the sensing part can be executed on the wearable device, whilst the sampled data must be sent out to mobile phones or PCs with the high computing capability needed for reconstruction and analysis. The authors of [34], [35] proposed a time-domain adaptive sampling framework to predict the next sampling point based on historical sampled data and therefore reduce the power overhead for signal reconstruction. However, though running is a relatively consistent motion from stride to stride, the in-stride signal is non-deterministic, changes quickly, and varies across runners. It is therefore not practical to build a generic running signal model to predict future samples.

To the best of our knowledge, Gazelle is the first wearable solution for online running form analysis with a primary focus on energy optimization driven by adaptive detection and consideration of the repetition and predictability of human running. Gazelle works in realtime out in the real world, and its performance and energy savings

Fig. 3. The example chest worn usage scenario of the Gazelle mobile running analysis system.

have been demonstrated through extensive in-lab experiments and outdoor use by real runners.

3 GAZELLE SYSTEM DESIGN

The Gazelle wearable system architecture is illustrated in Fig. 2. It consists of (1) a system-on-chip with a 16 MHz low-power ARM Cortex-M0 and BLE/ANT+ wireless interface, (2) a nine-axis MEMS IMU suite with high-precision, high-power accelerometer (HHA), and gyroscope, (3) a standalone ultra-low-power, low-precision accelerometer (LLA), (4) an ultra-low-power watchdog timer, (5) a system power management unit, and (6) a standard CR2032 225 mAh coin-cell battery.

With a form factor of 2 cm×3 cm×1 cm and less than 8 grams of total weight, Gazelle can be easily worn on different parts of a user's body, such as the chest, ankle, foot, or elsewhere. As shown in Table 1 below, depending on the specific worn body location, different running metrics can be obtained. Gazelle's wireless interface, enables communication with a sport watch or mobile phone, which can provide voice or visual feedback as illustrated in Fig. 3.

3.1 Hardware

Processing and Communication: With form factor being a primary design driver, minimizing PCB size and power consumption is a first order consideration in Gazelle's hardware design. The *nRF51422* is a System-on-Chip (SOC), equipped with a 32-bit ARM Cortex-M0 CPU and a 2.4 GHz ultra-low power RF front end. The RF front end supports concurrent Bluetooth Low Energy (BLE) and ANT+ protocol operation. The *nRF51422* allows on-board data processing and enables

TABLE 1
Key Running Form Metrics

Metric	Definition	Chest	Hip	Foot	Ankle	Wrist
Stride Time (ST)	Duration of a stride	Y	Y	Y	Y	Y
Ground Contact Time (GCT)	Duration foot is in contact with ground	Y	Y	Y	Y	N
Vertical Oscillation (VO)	Amount of bounce up and down	Y	Y	N	N	N

multi-platform (e.g., ANT+ Sport Watches & BLE Mobile Phones) data sharing. In addition, the *nRF51422* provides a flexible power management unit that can be used to further minimize power consumption. For example, depending on the user's usage pattern, Gazelle can switch between different states (e.g., idle or active).

Sensing: Measurement timing resolution (i.e., accuracy) and flexible sample rate control (i.e., power savings) are the two main driving factors in the design of the sensing hardware. Based on our studies of runners' walking and running signals, the maximum running acceleration can reach 16 g, which occurs when the foot strikes against the ground. We chose the *MPU9250* IMU as the main motion sensing unit because it is compact yet meets Gazelle's sensing precision requirements. The *MPU9250* includes an accelerometer and a gyroscope, supporting flexible individual sensor mode selection (e.g., standby, on/off), and quick adaption to changes in sensor sampling rate. However, one drawback of the *MPU9250* IMU is the high power consumption, e.g., 400 μA for the accelerometer in normal mode. Therefore, we added an ultra low power, lower accuracy accelerometer whose power consumption is two orders of magnitude less than that of the *MPU9250* IMU. The *ADXL362* (3 μA at 400 Hz and 1.1 μA motion activated wake-up mode) is used to detect user status and running form changes. The information gathered from the *ADXL362* drives the configuration of the high power IMU. This control process is discussed in more detail in Sections 3.2 and 5.4.2.

In addition to processing, sensing, and communication, 24/7 reliable operation is needed. Most of the time the system is idle in the OFF mode, and it continuously monitors the user's motion to trigger system wakeup. The *nRF51422* has an internal watchdog timer, but based on our testing, it was operational only in the higher current ON mode. Therefore, an external ultra low power 100 nA watchdog timer, the *PCF2123*, is incorporated to ensure system health while keeping accurate system time.

3.2 System Workflow

Gazelle's software is built on top of the *nRF51422*'s wireless protocol stack and SDK, taking less than 35 KB of flash memory. The software enables microsecond-resolution coordinated event-driven streaming operation, including system model checking, error handling, the operations of sensors, data processing, data storage, and wireless communication.

The Gazelle IMUs have built-in features to detect motion events, freeing the microprocessor from needing to actively read and process sensor data. For example, the ultra-low-power, lower-accuracy accelerometer *ADXL362* used in Gazelle can sample data and alert the microprocessor only when the acceleration has exceeded a predefined threshold for a predefined length of time. The microprocessor can keep track of time while in OFF mode between interrupts by reading the elapsed time of the watchdog timer. The microprocessor can dynamically change the threshold and time window in realtime. Taken together, an effective yet extremely low-power finite state machine classifier can be constructed. A simple rule-based approach can be used to classify user motion activity. To classify a walking/running pattern, the microprocessor can first configure the sensor to interrupt on a high-acceleration event, such as the impact

due to a user's ground strike. Then, the microprocessor can reconfigure the sensor to look for a lower acceleration event, the toe-off, to occur after a minimum expected time duration, i.e., the time the foot spends on the ground. Appropriate time window durations and acceleration thresholds are tuned with walking/running datasets representing the majority set of walkers/runners.

When the user's running motion is detected by the system's low power classifier, the sensing hardware is reconfigured to capture running signals in high resolution. Captured running signal features are used to drive the sparse adaptive sensing algorithm which 1) drives real-time IMU reconfiguration while running, and 2) constructs running metrics on board. Gazelle's wireless communication with either a sport watch or mobile phone is also triggered which allows the streaming of computed running form results to the user for on-the-fly feedback and post-run analysis.

The rest of the paper will focus on the proposed SAS algorithm to enable energy-efficient, high-resolution running form sensing and analysis.

4 MOBILE RUNNING ANALYSIS

Kinematic analysis is used to quantitatively assess human locomotion. Running and walking motions are periodic. Stride by stride, force is produced by multiple muscle groups propelling the body forward and upward, while maintaining body kinematic stability. Gait can be broken down into a repetitive series of strides. A set of kinematic metrics can be measured, and then the musculoskeletal functions can be quantitatively evaluated. In this section, we demonstrate that the Gazelle system can capture such metrics for running with high accuracy when compared with traditional laboratory high-speed video camera systems and force plates. We then motivate the sparse adaptive sensing algorithm, by identifying those features intrinsic to running that uncover opportunities for significant reduction of energy consumption without a significant impact on accuracy.

4.1 Gazelle Sensor Accuracy Validation

To verify the Gazelle accelerometer accuracy is sufficient for running form analysis in the field, comparative experiments were conducted in a physiology laboratory equipped with a Vicon camera system and a treadmill instrumented with force plates. The Vicon system consists of an array of eight high speed, high resolution cameras placed in a ring to fully encircle the treadmill and runner under test. At multiple biometric landmarks, e.g., the ankle, knee, and chest, the runner was equipped with an infrared reflector, and a Gazelle device.

In each experiment, Gazelle's high power accelerometer was sampled at 200 Hz while the Vicon cameras captured images at 200 fps and the force plate system ran at 1 kHz. Among the running metrics listed in Table 1, ST, GCT, and VO were each computed from raw Gazelle accelerometer data. To obtain ground truth for these metrics, data from the Vicon cameras and force plates system were processed as follows. Vertical oscillation was measured by subtracting the low to high points of the infrared reflector located on the runner's chest within each stride. Ground contact time was measured by computing the duration between foot touchdown and toe-off events. Touchdown and toe-off
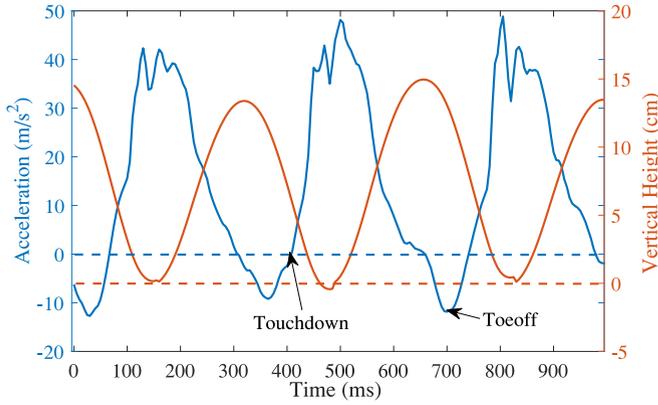
Fig. 4. Running stride acceleration from chest and vertical height.

Fig. 6. Error distribution for ST, GCT, and VO.

events were determined from force plate data by applying a threshold of 50 N for touchdown and 10 N for toe-off to the vertical force. Threshold in this range is recommended throughout the kinematic analysis literature to eliminate false detections due to force plate noise [36], [37], [38]. Stride time was obtained by subtracting step-by-step foot touchdown event. To extract those corresponding metrics from Gazelle, touchdown and toe-off events are also utilized. Fig. 4 shows a sample running acceleration collected from chest and the vertical height from acceleration integration. Touchdown event in the acceleration is identified by the zero-crossing right before the impact peak, and toe-off is identified as the negative minima after impact peak. Hence, ST and GCT can be computed in the same way as those obtained from force plates. VO is the difference between maximal height and minimal height, while vertical height is obtained by double-integrating the acceleration in which gravity is removed by a high pass filter.

The tests consisted of nine different speed and cadence settings: the cross product of 5 , 6 , and 7 mph speeds with
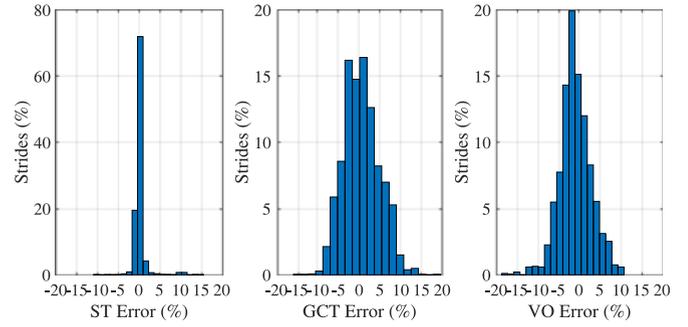
cadences of 160 , 175 , and 190 spm. Each setting was tested for 3 minutes in duration with the treadmill set for zero degrees of incline. In addition, a metronome was used during each test to assist runners to pace with the specified cadence. Gazelle was configured to stream raw data from HHA. In existing IMU-based kinematic analysis work [19], [20], [39], the IMU sampling rate can vary from 100 to 200 Hz, and at most 2,000 Hz, depending on the degree of subtlety the running-form metric of interest has. In our experiments, the HHA was configured to a 200 Hz sampling rate in order to sufficiently capture the running-form metrics. To compare the running metrics computed from Gazelle data to those computed from the sports physiology laboratory camera system data, the definition of accuracy in Eqn. (1) was used.

$$Accuracy = \frac{1}{N}\sum_{i=1}^{N}\left(1 - \frac{|M_G^i - M_L^i|}{|M_L^i|}\right)\times 100\%, \quad (1)$$

where M_G^i and M_L^i are the running metric for each stride i computed from data measured by Gazelle and the laboratory camera system respectively. Fig. 5 shows representative results from two study participants and Fig. 6 shows the error distributions from all speed settings for each
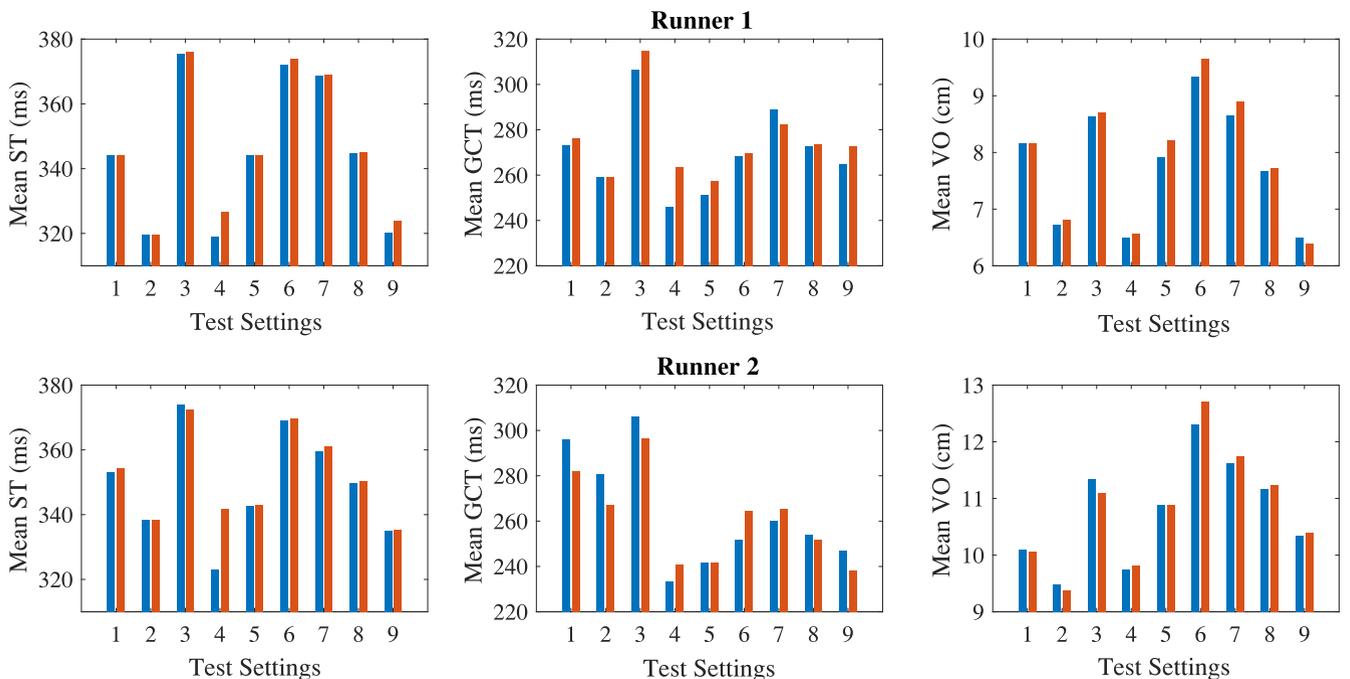

Fig. 5. Comparison of running form metrics captured by Gazelle and a physiology laboratory using Vicon camera and force plates system.

metric. This study demonstrates that when compared with the high-speed motion capture system, Gazelle offers over 99, 98, 97 percent accuracy on average for ST, VO, GCT respectively, at all nine test settings. The results from different settings illustrate that under changes of speed and cadence, Gazelle sensor has similar stability of system accuracy as the laboratory-grade systems.

4.2 Opportunities for Energy Savings

Energy efficiency is of utmost importance when supporting online running analysis with wearable sensors. Having demonstrated that Gazelle is able to achieve high accuracy with regular sampling of acceleration at 200 Hz, we now consider techniques to further reduce the number of samples, and therefore relax the energy requirement, while maintaining high accuracy. The challenge ahead is to answer the following two part question. *How many samples are minimally needed, and how to select the reduced sampling set?*

Stride-by-Stride Variance is Low. Running form typically changes gradually over time. In real-world running, it is unnecessary to provide user feedback stride-by-stride. Instead, feedback on running metrics can be provided only when a form change is detected, or at a user defined feedback interval. Therefore, it becomes possible to characterize the current running form by aggregating samples across many strides. Per stride, we can significantly reduce the required data sampling rate, thereby minimizing energy consumption, yet still maintain high running form analysis accuracy. This motivates our design of *sparse sensing (SS)*, which consists of three key steps: (1) detect running form changes and group strides with similar running form together, (2) sparsely sample data within the same stride group, and (3) reconstruct a single stride from the sparse samples within each stride group and compute the corresponding running metrics. Since the strides within each group have high similarity, the sparse samples we obtain from individual strides allow reconstruction of one representative stride for each stride group. Intuitively, there are two potential ways to get the representative stride: (1) Combine all samples to reconstruct a full stride signal and compute running metrics from it; (2) Since the results demanded by users are running metrics, metrics from selected strides in the same group can be computed and then the average for each metric can be calculated for user feedback.

Intra-Stride Variance is Predictable. Given known contextual information, such as the foot touchdown, the significant event patterns within each stride are predictable in time. From Fig. 4 in Section 4.1, we can see that, running acceleration is a periodic signal, and within one period, the signal changes sharply after the touchdown, while the change is more gradual around toe-off. Therefore, more samples are needed after touchdown, and less around toe-off, to capture sufficient information. The sampling rate can be adapted based on the variance pattern of running acceleration. Additionally, as is illustrated in Fig. 4, to compute ST, GCT, key points including consecutive zero-crossing points and minima are necessary to be captured. Therefore, instead of using a uniform high frequency sampling rate, we can: (1) change the sampling rate adaptively by detecting and predicting the local variance within a single stride; and (2) based on this prediction adaptively sample only the points

in time that are key to describe the selected running metrics of interest. The strategy for how to adaptively capture those key points varies based on a user's metric selection. For example, VO is computed through double integration of the acceleration signal, presenting a more challenging scenario. Therefore, the tradeoff between lost accuracy and power savings from adaptive sampling when compared with the fully sampled acceleration signal must be identified and minimized per metric. This motivates our design of *adaptive sensing (AS)*, and when combined with SS, *sparse adaptive sensing*, which consists of three key steps: (1) detect running form intra-variability, (2) adaptively adjust sampling rate based on the intra-variability, and (3) reconstruct a single running profile from the adaptive samples within a stride group and compute the corresponding running form metrics. Given the observations above, we conducted theoretical analysis to understand the feasibility and potential performance of both *sparse sensing* and *adaptive sensing*, which we present in Section 5.

5 SPARSE ADAPTIVE SENSING

This section describes Gazelle's sparse adaptive sensing, used to enable accurate and long-term running analysis under day-to-day real-world conditions. First, we examine the theory behind SAS, then detailing the implementation of SAS. Lastly, we report our experimental results, showing that SAS maintains high accuracy and performance even when delivering an energy savings of from 76.9 percent to up to 99 percent over the continuous high frequency sampling case.

5.1 Sparse Sensing

Human running acceleration signal can be represented in a sparse domain, e.g., using wavelets. Compressed sensing (CS) [31] can be used to estimate the number of samples required to reconstruct the signal. For example, we can derive the minimum number of samples required to ensure that the running metrics computed from the reconstructed running acceleration signal achieve ≥ 90 percent accuracy compared with that computed from the 200 Hz uniformly sampled signal, as follows. Given a signal $S \in \mathbf{R}^n$, we can first decompose it using wavelets basis $\Psi = [\psi_1 \psi_2 \ldots \psi_n]$, as shown in Eqn. (2).

$$S = \sum_{i=1}^{n} c_i \psi_i. \qquad (2)$$

Assuming ΨS is k sparse, the number of samples required for reconstruction satisfies the following inequality,

$$m \geq C \cdot \mu^2(\Phi, \Psi) \cdot k \cdot \log n, \qquad (3)$$

where C is a small positive constant and $\mu(\Phi, \Psi) = 1$. Then, $C \cdot k \cdot \log n$ samples are required for perfect signal recovery [31]. From our analysis, 5 percent (10 Hz on average) of the n samples need to be preserved to achieve 95 percent accuracy for ST, while around 25 percent (50 Hz on average) of the samples are needed to achieve 95 percent accuracy for GCT and VO. We therefore find theoretical opportunity to reduce sampling and processing energy overheads from 75 to 95 percent whilst maintaining 95 percent accuracy.
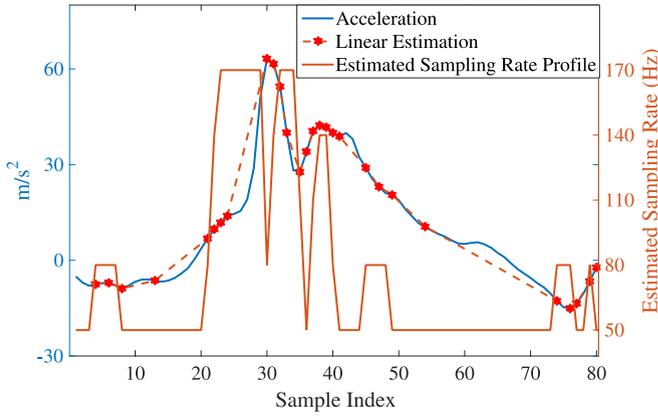
Fig. 7. Wavelet-based adaptive sampling rate estimation.

5.2 Adaptive Sensing

Measuring the *intra-variability* of a running stride is an essential step in sparse adaptive sensing. Intra-variability is a measure of the local variance of a signal. In order to quantify intra-variability for use to adaptively control sensor sampling rate, we use wavelets to analyze the adaptive sampling rate required for different segments inside a stride signal. As described in Section 5.1, running acceleration can be decomposed into wavelets. To estimate the sampling rate, the first step is decomposing the signal S as below to get the approximate and detailed wavelets coefficients c_{low} and c_{high} [40], [41],

$$c_{low} = (S * h) \downarrow 2 \qquad (4)$$

$$c_{high} = (S * g) \downarrow 2, \qquad (5)$$

c_{low} is then quantized in the range of 200 Hz to find adaptive sampling rates that correspond to the intra-variability of a running signal. Fig. 7 demonstrates a single stride acceleration, the estimated adaptive sampling rates over time, and reconstructed signal based on linear interpolation. The sampled and reconstructed result can be seen to visually correspond to the dynamic changes across the original signal. When applied to our dataset, the wavelet-based sampling rate estimation shows that in order to achieve 90 percent accuracy for the running metrics computed from the reconstructed signal, on average, 80 Hz sampling rate is needed.

5.3 Limitations of CS and Wavelets

Our analysis from Sections 5.1 and 5.2 shows that both *sparse sensing* and *adaptive sensing* can be utilized to reduce the sampling rate yet still maintain high accuracy for running form analysis. However, CS and wavelets adaptive sensing are computationally intensive and not well adapted to the running signal.

High Computational Complexity. According to [32], [33], the complexity for CS reconstruction ranges from $O(M^2 N^{1.5})$ to $O(\log(k)MN)$. Although the sparse sampling can be optimized to achieve only 5 percent CPU time for an 8 MHz wireless sensor node, the reconstruction required 30 percent CPU time on an *iPhone 3GS* with a 600 MHz processor [32], which is computationally intensive and not suitable for low-power CPUs. For runners who do not carry mobile phones, it is impractical to use CS on an ultra-low power
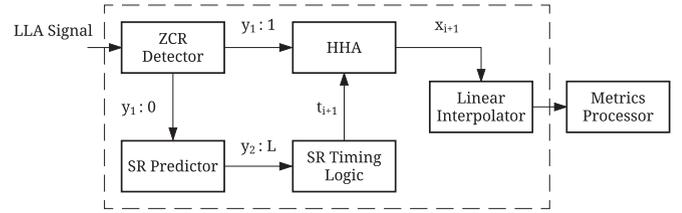

Fig. 8. SAS flow chart.

16 MHz CPU based wearable device. While the wavelets adaptive sensing reconstruction process can be as simple as performing a linear interpolation. To fit the restrictions of mobile kinematic analysis, we must further lower our reconstruction complexity.

Poor Real-Time Adaptability. Another limitation of CS or wavelets adaptive sensing is when transforming the time domain information to a sparse domain, both lack the ability to adaptively sample data based on running variability and the variability of a user's on-the-fly selection of running metrics of interest. For example, as demonstrated in Fig. 4, when only GCT is of interest to a runner, CS and wavelets adaptive sensing are not able to capture only the key points for computing GCT to achieve optimal sampling rate. Moreover, wavelets adaptive sensing requires offline processing with all signals known beforehand to build a sampling rates model, which works for efficient data storage and transmission, but is not feasible to reduce samples in realtime and hence to reduce power consumption from sensing.

Additionally, based on the analysis in Sections 5.1 and 5.2, the required sampling rate is not low enough to achieve high energy reduction. Therefore, both methods are not well suited for realtime adaption to a real world running signal, presenting key barriers to their use in a power-aware, low-profile wearable system.

5.4 SAS Algorithm Design

An alternative to overcome the limitations in Section 5.3 is to conduct all the analysis in the time domain and design an easily-configurable sensing algorithm which can adaptively optimize power and accuracy across the running metrics of interest. In this work, we have designed the SAS algorithm using direct time domain analysis to avoid the high computation complexity of time-frequency domain transformation and reconstruction processes, while preserving real time adaptivity to different running metrics, thus enabling a novel and highly energy efficient long-term running form analysis on the Gazelle wearable device. Fig. 8 shows the overall SAS work flow. A zero-crossing (ZCR) detector and a sampling rate predictor (SRP) are used together to control HHA, and a linear interpolator is applied to reconstruct the samples from the HHA. The detailed design and implementation process is described in the following sections.

5.4.1 SAS Design

The first question to tackle in the SAS flow is when to opportunistically acquire the next needed sample from the HHA. The largest time interval t_{i+1} between samples with the minimal loss in information is desirable. As mentioned earlier, the dependence lies on the variance pattern of the acceleration signal. The time interval can be chosen such
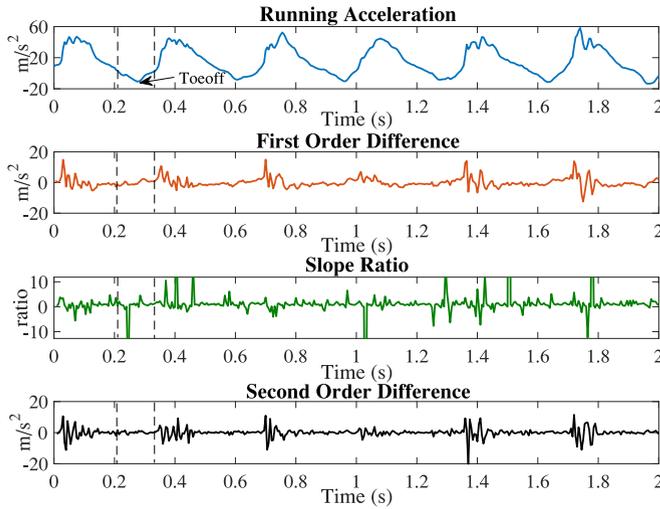
Fig. 9. SAS features.

that only the most critical points are captured for signal reconstruction. Thus we propose a method to determine an optimized t_{i+1}. First, we assume there is a finite set of intervals $\{T_1, T_2, \ldots, T_l\}$ to select from. Then, by constructing a projection from the predicted variance of the signal to the set of time intervals, the interval t_{i+1} can be determined. To predict which T_l should be used to acquire the next sample from the HHA, the local variance of the signal from the LLA, sampling at a higher frequency than the maximum HHA frequency, is utilized for prediction. To measure the LLA variance, three features are examined: (1) *first-order difference (FOD)*, (2) *slope ratio (SRO)*, and (3) *second-order difference (SOD)*. FOD measures the sharpness of positive or negative slopes, SRO captures inflection points including local minima and maxima, and SOD estimates the slope rate of change. The FOD, SRO, and SOD features are computed as follows:

$$FOD = x_i - x_j \tag{6}$$

$$SR = \frac{(x_i - x_j)/(i - j)}{(x_j - x_k)/(j - k)} \tag{7}$$

$$SOD = FOD(i) - FOD(i - 1). \tag{8}$$

Fig. 9 shows all three features along with running acceleration. FOD and SOD are sensitive to LLA acceleration when the foot is in contact with the ground, where most acceleration variance occurs. Additionally, we compared the standard deviation of FOD and SOD for the segment in each stride (between the two vertical dashed lines in Fig. 9) around toe-off events. Compared with SOD, FOD has higher standard deviation and hence more sensitive around toe-off events. Because FOD has less computation overhead and can cover those minima, maxima points that are primarily covered by SRO, FOD is preferred for driving the SR Predictor. However, signal variance around zero-crossings is not significant enough for FOD alone to predict critical samples; the zero-crossing points are often missed. Thus the ZCR Detector is added to augment the prediction. Combining the ZCR Detector and SR Predictor, high accuracy for all running metrics can be achieved.

Next, a set of proper sampling intervals, which can be considered as the pseudo sampling frequencies, is determined for the HHA. Here we refer to the multiplicative inverse of sampling intervals as pseudo sampling rates. This is because in practice, an accelerometer sensor may not support the actual sampling rate needed. One-shot operation is therefore utilized to attain the requisite pseudo sampling rate. A similar approach is used in the work of Feizi et al. [42], where the authors proposed the TANS with finite sample rate (TFR) method. In their work, an offline electrocardiograph (ECG) signal was divided into three repeating states, whereby each state was strictly assigned a minimally needed sampling rate. TFR requires, for each state, a known signal starting point and approximate number of samples for each state. Although running acceleration and ECG are both periodic, running acceleration has higher variance from stride to stride when compared with beat to beat variance in ECG. For example, higher sampling rate may be required when a runner runs on a hard ground during ground contact time, while a lower sampling rate may be required when running on grass. Assigning a fixed sampling rate to a fixed segment within a stride of running acceleration, as done in TFR, limits the lowest sampling rate that can be achieved and not well adapts to the stride by stride running signal. Numerically, there are infinite combinations of possible HHA pseudo sampling rates. However, based on the target running signal, there are other further constraints: (1) The minimal sampling rate needs to ensure at least one sample can be obtained within a stride, and (2) the maximal pseudo sampling rate cannot exceed the sensor's maximal sampling rate with the consideration of the HHA sensor's measured startup delay. With those constraints in the design process, we further propose an empirical design criteria for the SR Predictor: We must minimize the number of sampling rates based on the patterns of the SR Predictor. For example, the FOD feature shown in Fig. 9 has the following clear patterns: (1) flat signal appearance and (2) dynamic signal changes with high amplitude. Therefore in our experiments in Section 6, two different boundary sampling rates are used. With this criteria and constraints identified, a set of pseudo sampling rates can be determined using the training data. The resulting average pseudo sampling rate therefore must satisfy the following equation:

$$\bar{sr} \le \frac{(N_{T_m} \cup N_{zcr} \cup N_{T_t})}{\sum_{i=1}^{N} ST_i}, \tag{9}$$

where N_{T_m} is the number of samples obtained with minimal interval T_m in the set $\{T_1, T_2, \ldots, T_l\}$, and N_{zcr} is the number of zero-crossing points. And, N_{T_t} is the number of transitions between any two different consecutive intervals. This augment to the SR Predictor design is based on the assumption that when an interval transition occurs, the samples close to this transition are important for describing the signal.

Fig. 10 demonstrates the reconstructed signals from the SAS algorithm as compared with the compressed sensing method. The original 200 Hz signal was reduced to an average of 30 Hz for both algorithms. As can be clearly observed in the figure, SAS outperforms CS with a lower mean squared error of 17.70. While CS can recover the overall shape and periodicity of the original signal, it does so with
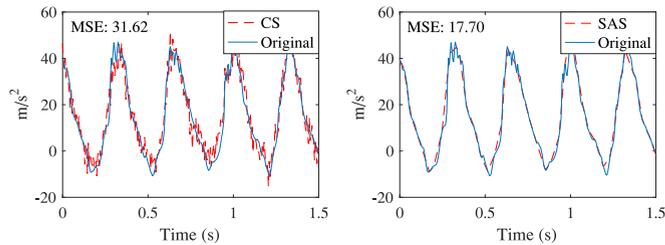
Fig. 10. Reconstructed signals from CS and SAS.

much lower signal to noise ratio. In Section 6.1, further comparison between SAS and CS are conducted.

5.4.2 SAS Implementation

As described in Section 3, Gazelle is equipped with a low-accuracy, ultra-low-power accelerometer (LLA) and a high-accuracy, high-power accelerometer (HHA). The LLA samples continually throughout a run. Even though the LLA suffers from high noise, it offers sufficient accuracy to continually detect the stride-by-stride timing structure and to estimate the similarity of running strides with low latency. Also, even though the LLA sensor cannot provide absolute accuracy for its acceleration measurement, velocity, or position related metrics, it offers sufficient relative accuracy to detect changes of these metrics, and thus the change of running form.

Algorithm 1. SAS Algorithm

1:    $levels$ {sampling rates look-up table}
2:    $maxSr$ {maximal sampling rate in $levels$}
3:    $preSr \leftarrow newSr$ {update previous sampling rate}
4:    **for all** newSample from LLA **do**
5:      **if** zero-crossing detected **then**
6:        Get a sample from HHA
7:      **else**
8:        get recent three $|fods|$
9:        $fodMax \leftarrow max(|fods|)$
10:        **if** $fodMax > preMax$ {find maximal $|fod|$} **then**
11:          $preMax \leftarrow (\lambda) \times fodMax + (1 - \lambda) \times preMax$
12:        **end if**
13:      **end if**
14:      $newSr \leftarrow (fodMax/preMax) \times maxSr$
15:      look up closest sampling rate in $levels$
16:      **if** $preSr \neq newSr$ **then**
17:        **if** $|lastHHA - curLLA| > thr$ **then**
18:          Get a sample from HHA
19:        **end if**
20:      **else**
21:        Sample with $newSr$
22:      **end if**
23:    **end for**

The LLA consumes 3 μA and samples data at 400 Hz, in order to detect zero-crossings and estimate sampling rate beforehand, which are used to notify the host processor of such events. Although past work has shown lower sampling rates can be sufficient for accurate kinematic analysis, sampling the LLA at lower frequencies (1) negligibly improves battery life (e.g., 1.8 μA sampling at 100 Hz saves 0.5 percent of *CR2032* capacity per 1,000 hours of activity), and (2) reduces system accuracy by increasing the latency

to trigger the sampling of the HHA. In order to ensure the HHA's sampled data is able to catch the acceleration feature detected by the LLA, the delay from both the LLA trigger and the startup time from the HHA must be lower than the sampled signal's bandwidth in Hz. From past work, a commonly used acceleration signal sampling frequency for low-power kinematic analysis is 100 Hz. Therefore, a delay from acceleration feature to LLA trigger to HHA sampling of 10 ms or less will lose minimal fidelity. Due to this constraint, utilization of angular velocity data sensed by a gyroscope is not usable in the adaptive SAS algorithm as typically gyroscopes require 20 to 80 ms for start up. One solution to utilize a gyroscope with reduced power is by applying a constant duty-cycle. Due to space constraints, we do not consider such use of the gyroscope in this work. Operating the LLA at 400 Hz yields a 2.5 ms sampling delay, leaving up to 7.5 ms for HHA start up time to observe the 10 ms boundary. Therefore, we must find an accelerometer which can satisfy the start-up time constraint while maintaining high accuracy. While data from the *MPU9250* was used for the HHA during our algorithm design, the high precision accelerometer from the *MPU9250* has a maximal 25 ms startup time from sleep mode to active mode, which would then violate this constraint under a real-time implementation. Therefore the HHA used in the pilot study, which provides "first sample correct" and "zero-delay" capabilities, is the *LSM6DS3* [43]. The LSM6DS3 was measured to have a 2.38 ms delay from the start of SPI configuration commands while in power down mode to the first activated data ready interrupt signal, thereby meeting the overall real-time 10 ms constraint for signal feature to HHA sampling time delay interval.

The samples obtained by the LLA are then used to detect zero-crossings and predict pseudo sampling rates for this HHA used in our study. To achieve the adaptive selection of pseudo sampling rates, the most recent three consecutive absolute values of FOD are computed, and the maximal absolute FOD value is scaled by a global maximal absolute FOD. The scaled value is then used for looking up a proper pseudo sampling rate or time interval, as described in Algorithm 1. The HHA is then brought out of the power down mode and configured for operation at 400 Hz, and the first available sample is then acquired from HHA, achieving the selected pseudo sampling rate. The pseudo sampling rate is again updated when the absolute difference between the last HHA sample and current LLA sample exceeds a threshold. This threshold is optional, and only used when lower average sampling rate is necessary. Setting the threshold to a low value can ensure key points are captured while reducing redundant points. For example, in Section 6.1, the threshold is set to 1.8 m/s^2. Additionally, a low pass filter can be applied to the global maximal absolute FOD to smoothly adapt to local changes in acceleration. Algorithm 1 summarizes the full SAS procedure.

Using the samples captured by our SAS algorithm, reconstruction methods can be applied to recover the running profile to compute all the running form metrics. Specifically, reconstruction is necessary because vertical oscillation double-integration of the single stride signal. In this paper, we choose linear interpolation as reconstruction method, which has low complexity, enabling on-board reconstruction. Note
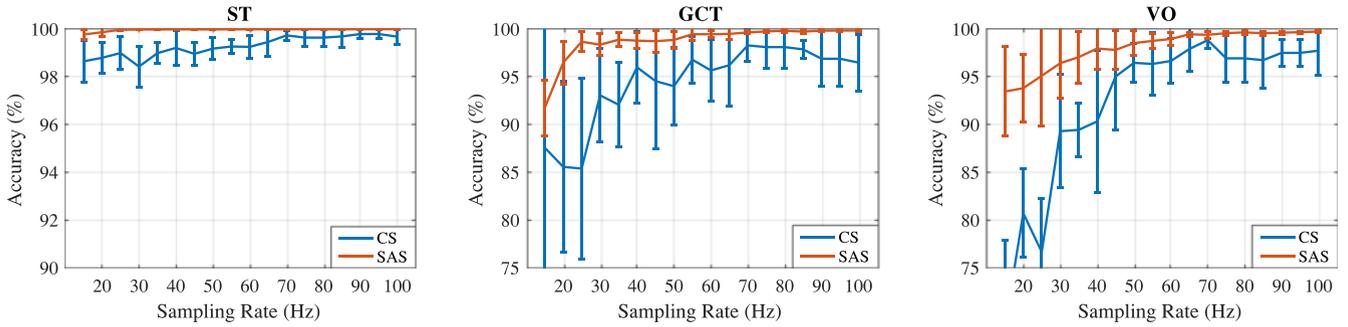
Fig. 11. Running metrics accuracy comparison between CS and SAS.

that the LLA is also used to estimate stride-by-stride running form changes based on stride time, and this information is used to group similar strides together to further reduce sampling rate. For example, if every stride inside a group is close to the mean stride and runner does not require stride-by-stride feedback, essentially, only one running stride needs to be processed to provide the running form metrics. However, as we will show in Section 6.2, the actual amount of energy saving depends on a runner's consistency, which varies by the experience and fitness of a runner.

6   EVALUATION

To evaluate the energy efficiency and accuracy of the Gazelle wearable system for online running analysis, we conducted both in-lab experiments of the SAS algorithm and in-field pilot studies.

6.1   In-Lab Experiments

For the in-lab experiments, we first compared the accuracy of our proposed SAS algorithm with that of the compressed sensing. Although, due to the intensive computation cost of CS, CS is not an optimal option for on-board sampling rate reduction without sufficient hardware support, CS is the leading approach to achieve high accuracy with a low sampling rate. Thus, in this experiment, we primarily compare SAS and CS from the perspective of reconstruction accuracy. In the experiment, seven 30 minute-long running datasets were recorded on an outdoor track. Each runner wore a chest band with the Gazelle device attached to the band in the center front location. In the test, both real-time running metrics and raw acceleration samples collected from HHA were streamed to a mobile phone for post validation. The key running metrics: ST, GCT, VO were computed as a comparative baseline from the raw data sampled from HHA over the entire running test. To determine the general trade-offs between sparse (adaptive) sensing rates and energy savings, we computed the average accuracy using stride-by-stride running form metrics, which did not include the added benefits of grouping similar strides together. The accuracy was defined as

$$Accuracy_{avg} = \frac{1}{N} \sum_{n=1}^{N} \left(1 - \frac{|M_{\{a\}}^n - M^n|}{|M^n|} \right), \qquad (10)$$

where $M_{\{a\}}$ is the metric computed from either SAS or CS resulted running signal, M^n is the metric computed from full 200 Hz sampled running signal. $n = 1, 2 \ldots N$ is the index of each stride for a specific running metric.

For CS, the sampling rate was fixed for each experiment; while for SAS, the sampling rate changed dynamically and the average sampling rate was used for comparison. With the results from Fig. 11, it can be referred that SAS outperforms CS in term of achieving lower sampling rate with sufficient accuracy, provide more potential to reduce energy consumption either for online signal processing or wireless transmission. Fig. 11 compares the accuracy between CS and SAS for different running metrics under different sampling rates of the HHA. We can see that SAS outperforms CS in almost all the scenarios. For ST, GCT, and VO, an average sampling rate of 25 Hz is sufficient to maintain higher than 99.0, 98.6, and 95.1 percent accuracy respectively, and this is sufficient for runners' feedback. Compared with our SAS method, CS achieves comparable accuracy for stride time, but has worse performance for GCT and VO, and cannot obtain an average of 90 percent accuracy when the sampling rate is lower than 30 Hz and 40 Hz, respectively. The major reason is demonstrated in Fig. 10: CS has much lower signal to noise ratio, and therefore error is accumulated when aggregating the ground contact time, and as vertical oscillation requires double integration, error is further accumulated.

We also conducted power modeling and analysis to determine the energy savings of the SAS approach as compared with the constant 200 Hz approach. Shown in Fig. 12, the current per sample was computed for SAS so we can
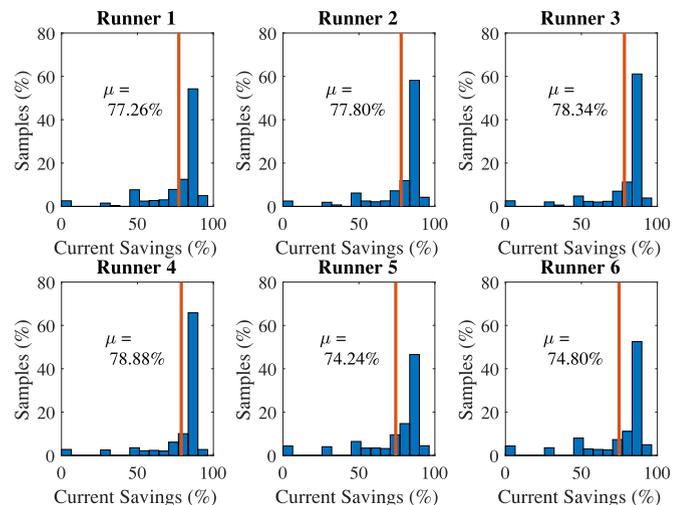

Fig. 12. Distributions of sample-by-sample current savings of adaptive SAS LLA + HHA sampling compared to constant 200 Hz HHA sampling, across 30 minute running sessions from six runners.
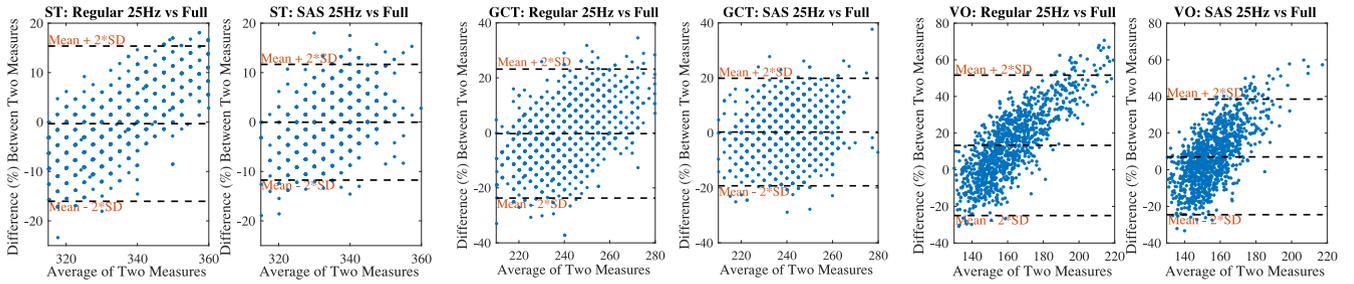
Fig. 13. Bland-Altman plots for regular 25 Hz sampling and SAS algorithm.

compare the resulting dynamic sampling rate of the HHA and the static 3 μA of the LLA. The average current per sample of the HHA can be computed as a combination of the current cost for a single conversion of the HHA in high-resolution mode (240 μA) over the HHA start-up time, and the HHA power-down current cost (6 μA) for the remainder of the sampled interval time for that sample. Overall, a average of 25 Hz sampling rate is required for SAS to achieve greater than 97.7 percent accuracy for all running metrics with over 76.9 percent energy savings. This represents one order of magnitude improvement over existing wearable running analysis devices, while outperforming CS in accuracy and achieving significantly lower computational overhead by operating exclusively in the time domain. To further validate the effectiveness of SAS algorithm at 25 Hz, we compared its performance with the regular 25 Hz sampling approach. Figs. 13 and 14 demonstrates that: (1) Regular 25 Hz sampling results in comparable average accuracy compared with SAS algorithm at 25 Hz, however, it has larger error range and its performance varies significantly from stride to stride. (2) The regular 25 Hz sampling method has more than 7 percent error in average for VO

than SAS algorithm. The reason is that regular 25 Hz sampling is not able to capture most of minima or maxima at sharp transitions. Thus, an adaptive, irregular sampling strategy like the SAS algorithm we proposed is necessary to reduce energy consumption while maintain high measurement accuracy.

In addition, in an actual usage scenario, runners may have different demands of running metrics, thus the maximum energy savings can vary for different metric subsets. For example, for stride time alone, the LLA active in interrupt-only mode is sufficient to capture these metrics at a 10 Hz sampling rate, and the energy savings can reach 99 percent compared with 200 Hz HHA. In future work, different usage scenarios can be studied. As shown, different running metrics require a different sampling rate to reach an accurate enough measurement. Therefore SAS can be designed to adapt to different sets of running metrics to further minimize the power consumption under various usage cases. In summary, our sparse adaptive sensing algorithm is energy-efficient and accurate for running form analysis and feedback, and provide a solution for long term running form study, and a potential guide for other similar applications.

Note that the accuracy and energy saving numbers above are for stride-by-stride running form analysis. Further sampling rate reduction can be achieved by grouping strides with similar running profile, which depends on how consistently the runner is running. Next, we further evaluate the energy savings from runners with different experience levels based on pilot studies in real-world running races.
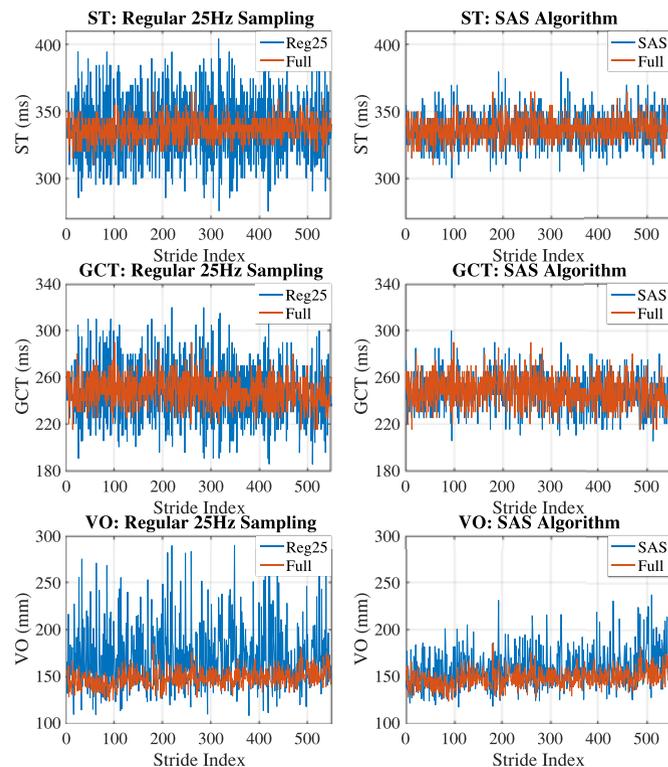
6.2 Pilot Study

In addition to laboratory testing and outdoor track testing, Gazelle was used in the Ironman World Championships in October 2014 Kona, Hawaii, the world's premier Ironman race event. In Kona, Gazelle monitored the marathon segments of two professional triathletes and six of the world's best athletes in their age brackets. This section will focus on reporting and analyzing Gazelle's results for the eight athletes from this race. The focus of this pilot study was twofold: 1) to test consistency of the metrics derived from the Gazelle wearable under the energy savings with SAS achieved in real world running; and, 2) to understand Gazelle's metrics' overall usability in terms of running form information representation when compared across some of the world's best triathletes under race conditions.

Energy Savings in Real World Running. Stride-by-stride running-form consistency affects the performance and the energy savings of SAS. As described in the previous section, across 10 runners data collected during in-lab experiments, an average of 25 Hz sampling rate was needed to achieve

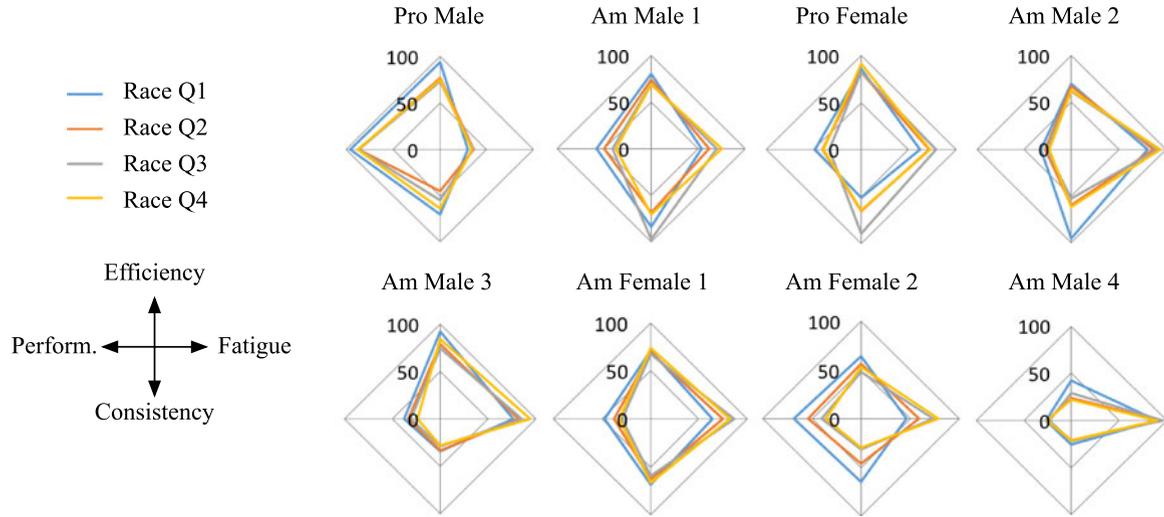Fig. 14. Stride by stride performance.

Fig. 15. Gazelle running analytics for top professional and elite triathletes at the Ironman World Championships in Kona, HI.

over 97 percent accuracy for all computed running form metrics. Running-form consistency varies among runners. Under the same stride time variance constraint, better running-form consistency leads to larger number of strides per group, hence lower data sampling rate and better energy savings. Fig. 16 shows the number of groups and the number of strides per group for each runner with 1 percent stride time variance. From this figure, Runner 1 shows the highest running-form consistency or minimal stride-by-stride variance, which leads to the largest number of strides per group, hence the lowest data sampling rate (1 Hz), and therefore largest energy savings (84.3 percent). On the other hand, Runner 7 shows the lowest running-form consistency, requiring the highest average data sampling rate (5 Hz), and resulting in the lowest energy savings (82.6 percent). Overall, an average energy savings of 83.6 percent was achieved across these eight runners.

Metric Report Consistency. Based on the high-level metrics shown Fig. 15, the averaged RunQuality scores for all eight runners are summarized in Table 2 along with each of their race completion times. It can be seen that based on the race time, the runners can be classified into four run skill levels, and the *RunQuality* derived from the run form metrics measured by Gazelle is highly consistent with runners' actual race results, as well as the associated energy savings from Gazelle. This comparison serves to validate the feasibility and methodology of Gazelle wearable under real world use. The following equations describe the high-level metrics, which are constructed post-race in terms of Gazelle's reported running metrics.

- $Efficiency = \frac{1}{t_{air} \times pace}$, *Efficiency* estimates how much energy is spent to propel the runner over the distance traveled.
- $Fatigue = \frac{t_{ground}}{t_{air}}$, *Fatigue* is an estimate of how tired the runner is.
- $Performance = Mean(\frac{t_{air}}{t_{ground}})$, *Performance* is an estimate for how much energy a runner is putting into the ground.
- $Consistency = StdDev(\frac{t_{air}}{t_{ground}})$.

Taken together, *RunQuality* is an aggregated measure of all the four high-level metrics described above. It is a simple unity weighted combination of the four, with the desirable set {*Efficiency, Consistency, Performance*} having positive unity weight and the undesirable set {*Fatigue*} having negative unity weight. The summation of the two sets together is a runner's RunQuality metric

$$RunQuality = Efficiency + Consistency + Performance - Fatigue.$$

In the weeks following the Ironman World Championships at Kona, athletes and their coaches reviewed the running form metrics data that were generated by Gazelle. The feedbacks we received were consistent among most athletes and coaches that Gazelle was easy to use and the running form metrics were useful for both understanding the precise places in the race where unexpected events
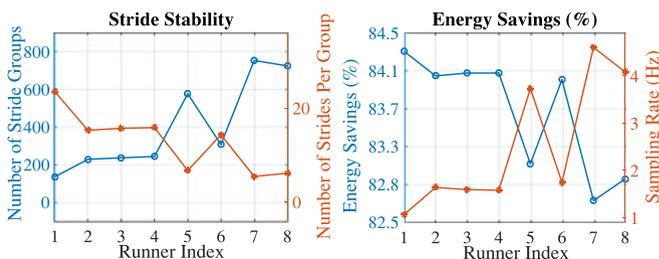

Fig. 16. Stride stability versus energy savings for eight different runners in the Kona Ironman World Championships.

TABLE 2
RunQuality Scores versus Race Time

Runner	RunQuality	Race Time	Level
Pro Male	90.3	2 h:58 m:58 s	4
Am Male 1	85.6	3 h:14 m:12 s	3
Pro Female	86.2	3 h:21 m:34 s	3
Am Male 2	80.6	3 h:41 m:51 s	2
Am Male 3	74.7	3 h:41 m:51 s	2
Am Female 1	80.5	3 h:52 m:38 s	2
Am Female 2	75.0	4 h:07 m:16 s	2
Am Male 4	62.5	5 h:02 m:54 s	1

occurred and for further improvement of the athletes' running form and racing strategy.

7 CONCLUSIONS

In this work, we have designed and developed *Gazelle*, a wearable system targeting long-term, online running form analysis. Gazelle leverages small economical sensors to ensure low cost, compact form factor, and light weight. To tackle the challenges associated with the high energy consumption of high-precision motion sensing and analysis, we have developed an intelligent sparse adaptive sensing and running form analysis solution, along with aggressive energy management techniques. Experiments using real-world running data demonstrate that, compared with uniform sensing at 200 Hz, SAS can achieve 97.7 percent accuracy and 76.9 percent energy saving with only an 25 Hz maximal sampling rate. As a result, together with the improvement in usable energy capacity due to lower average current draw, Gazelle can increase the battery life by one order of magnitude using a small coin-cell battery. Through our year-long pilot studies, Gazelle has been in use by over a hundred elite and recreational runners during day-to-day training and various racing events, with satisfactory results. Gazelle is in the process of being commercialized.

REFERENCES

[1] 80 million European runners reveal their reasons to run, (2009). [Online]. Available: http://www.prnewswire.com/news-releases

[2] Number of people who went jogging or running with the last 12 months in the United States, (2015). [Online]. Available: http://www.statista.com/statistics/227423/number-of-joggers-and-runners-usa

[3] A. Daoud, G. J. Geissler, F. Wang, J. Saretsky, Y. A. Daoud, and D. E. Lieberman, "Foot strike and injury rates in endurance runners: A retrospective study," *Med. Sci. Sports Exercise*, vol. 44, pp. 1325–1334, 2012.

[4] O. Fischer and W. Braune, *Der Gang des Menschen: Versuche am Unbelasteten und Belasteten Menschen*, Berlin, Germany: Hirzel Verlag, 1985.

[5] J. Bonacci, et al., "Running in a minimalist and lightweight shoe is not the same as running barefoot: A biomechanical study," *British J. Sports Med.*, vol. 27, pp. 387–392, 2013.

[6] C. Strohrmann, H. Harms, and G. Tröster, "Out of the lab and into the woods: Kinematic analysis in running using wearable sensors," in *Proc. 13th Int. Conf. Ubiquitous Comput.*, 2011, pp. 119–122.

[7] C. Strohrmann, M. Rossi, B. Arnrich, and G. Troster, "A data-driven approach to kinematic analysis in running using wearable technology," in *Proc. 9th Int. Conf. Wearable Implantable Body Sensor Netw.*, 2012, pp. 118–123.

[8] A. Muro-de-la Herran, B. Garcia-Zapirain, and A. Mendez-Zorrilla, "Gait analysis methods: An overview of wearable and non-wearable systems, highlighting clinical applications," *Sensors*, vol. 14, no. 2, pp. 3362–3394, 2014.

[9] M. Sousa, A. Techmer, A. Steinhage, C. Lauterbach, and P. Lukowicz, "Human tracking and identification using a sensitive floor and wearable accelerometers," in *Proc. IEEE Int. Conf. Pervasive Comput. Commun.*, 2013, pp. 166–171.

[10] D. E. Lieberman, et al., "Foot strike patterns and collision forces in habitually barefoot versus shod runners," *Nature*, vol. 463, pp. 531–535, 2010.

[11] T. Ashok and A. P. Sanjay, "Kinematic study of video gait analysis," in *Proc. Int. Conf. Ind. Instrum. Control*, 2015, pp. 1208–1213.

[12] C. Prakash, A. Mittal, R. Kumar, and N. Mittal, "Identification of spatio-temporal and kinematics parameters for 2-D optical gait analysis system using passive markers," in *Proc. Int. Conf. Advances Comput. Eng. Appl.*, 2015, pp. 143–149.

[13] P. O. Riley, G. Paolini, U. D. Croce, K. W. Paylo, and D. C. Kerrigan, "A kinematic and kinetic comparison of overground and treadmill walking in healthy subjects," *Gait Posture*, vol. 26, no. 1, pp. 17–24, 2007.

[14] J. R. Watt, J. R. Franz, K. Jackson, J. Dicharry, P. O. Riley, and D. C. Kerrigan, "A three-dimensional kinematic and kinetic comparison of overground and treadmill walking in healthy elderly subjects," *Clinical Biomechanics*, vol. 25, no. 5, pp. 444–449, 2010.

[15] N. Kane, M. C. Simmons, D. John, D. L. Thompson, and D. R. Bassett, "Validity of the Nike+ device during walking and running," *Int. J. Sports Med.*, vol. 31, no. 2, pp. 101–105, 2010.

[16] M. Milosevic, A. Milenkovic, and E. Jovanov, "mHealth@UAH: Computing infrastructure for mobile health and wellness monitoring," *Crossroads ACM Mag. Students-Wearable Comput.: Getting Dressed Tech*, vol. 20, no. 2, pp. 43–49, 2013.

[17] J. P. Porta, D. J. Acosta, A. N. Lehker, S. T. Miller, J. Tomaka, and G. A. King, "Validating the Adidas miCoach for estimating pace, distance, and energy expenditure during outdoor over-ground exercise accelerometer," *Int. J. Exercise Sci.*, vol. 2, no. 4, 2012, Art. no. 23.

[18] J. A. Noah, D. K. Spierer, J. Gu, and S. Bronner, "Comparison of steps and energy expenditure assessment in adults of Fitbit tracker and Ultra to the Actical and indirect calorimetry," *J. Med. Eng. Technol.*, vol. 37, no. 7, pp. 456–462, 2013.

[19] T. Liu, Y. Inoue, K. Shibata, and K. Shiojima, "Three-dimensional gait analysis system with mobile force plates and motion sensors," in *Proc. 8th Int. Conf. Ubiquitous Robots Ambient Intell.*, 2011, pp. 107–110.

[20] C. Senanayake and S. Senanayake, "Human assisted tools for gait analysis and intelligent gait phase detection," in *Proc. Innovative Technol. Intell. Syst. Ind. Appl.*, 2009, pp. 230–235.

[21] J. Bae, "Gait analysis based on a hidden Markov model," in *Proc. 12th Int. Conf. Control Autom. Syst.*, 2012, pp. 1025–1029.

[22] W. Xu, M.-C. Huang, N. Amini, J. J. Liu, L. He, and M. Sarrafzadeh, "Smart insole: A wearable system for gait analysis," in *Proc. 5th Int. Conf. Pervasive Technol. Related Assistive Environments*, 2012, pp. 181–184.

[23] Y. Wang, et al., "A framework of energy efficient mobile sensing for automatic user state recognition," in *Proc. 7th Int. Conf. Mobile Syst. Appl. Services*, 2009, pp. 179–192.

[24] A. Benbasat and J. Paradisio, "Design of a real-time adaptive power optimal system," in *Proc. IEEE Sensors*, Oct. 2004, vol. 1, pp. 48–51.

[25] Z. Yan, V. Subbaraju, D. Chakraborty, A. Misra, and K. Aberer "Energy-efficient continuous activity recognition on mobile phones: An activity-adaptive approach," in *Proc. 16th Int. Symp. Wearable Comput.*, 2012, pp. 17–24.

[26] S. Kang, et al., "Seemon: Scalable and energy-efficient context monitoring framework for sensor-rich mobile environments," in *Proc. 6th Int. Conf. Mobile Syst. Appl. Services*, 2008, pp. 267–280.

[27] K. Lorincz, et al., "Mercury: A wearable sensor network platform for high-fidelity motion analysis," in *Proc. 7th ACM Conf. Embedded Netw. Sensor Syst.*, 2009, vol. 9, pp. 183–196.

[28] R. K. Ganti, P. Jayachandran, T. F. Abdelzaher, and J. A. Stankovic, "SATIRE: A software architecture for smart attire," in *Proc. 4th Int. Conf. Mobile Syst. Appl. Services*, 2006, pp. 110–123.

[29] S. Zhu, H. Anderson, and Y. Wang, "Reducing the power consumption of an IMU-based gait measurement system," in *Proc. Advances Multimedia Inf. Process.*, 2012, pp. 105–116.

[30] T. Park, J. Lee, I. Hwang, C. Yoo, L. Nachman, and J. Song, "E-Gesture: A collaborative architecture for energy-efficient gesture recognition with hand-worn sensor and mobile devices," in *Proc. 9th ACM Conf. Embedded Netw. Sensor Syst.*, 2011, pp. 260–273.

[31] E. Candes and M. Wakin, "An introduction to compressive sampling," *IEEE Signal Process. Mag.*, vol. 25, no. 2, pp. 21–30, Mar. 2008.

[32] K. Kanoun, H. Mamaghanian, N. Khaled, and D. Atienza, "A real-time compressed sensing-based personal electrocardiogram monitoring system," in *Proc. Des. Autom. Test Europe Conf. Exhibition*, 2011, pp. 1–6.

[33] A. Dixon, E. G. Allstot, D. Gangopadhyay and D. J. Allstot, "Compressed sensing system considerations for ECG and EMG wireless biosensors," *IEEE Trans. Biomed. Circuits Syst.*, vol. 6, no. 2, pp. 156–166, Apr. 2012.

[34] S. Feizi, V. Goyal, and M. Médard, "Locally adaptive sampling," in *Proc. 48th Annu. Allerton Conf. Commun. Control Comput.*, 2010, pp. 152–159.

[35] S. Feizi-Khankandi, V. K. Goyal, and M. Médard, "Time-stamp-less adaptive nonuniform sampling for stochastic signals," *IEEE Trans. Signal Process.*, vol. 60, no. 10, pp. 5440–5450, Oct. 2012.

[36] P. G. Weyand, D. B. Sternlight, M. J. Bellizzi, and S. Wright, "Faster top running speeds are achieved with greater ground forces not more rapid leg movements," *J. Appl. Physiology*, vol. 89, no. 5, pp. 1991–1999, 2000.

[37] W. Sparrow and O. Tirosh, "Identifying heel contact and toe-off using forceplate thresholds with a range of digital-filter cutoff frequencies," *J. Appl. Biomechanics*, vol. 19, no. 2, pp. 178–184, 2003.

[38] C. F. Munro, D. I. Miller, and A. J. Fuglevand, "Ground reaction forces in running: A reexamination," *J. Biomechanics*, vol. 20, no. 2, pp. 147–155, 1987.

[39] D. Rodríguez-Martín, C. Pérez-López, A. Samà, J. Cabestany, and A. Català, "A wearable inertial measurement unit for long-term monitoring in the dependency care area," *Sensors*, vol. 13, no. 10, pp. 14079–14104, 2013.

[40] M. Petkovski, S. Bogdanova, and M. Bogdanov, "A simple adaptive sampling algorithm," in *Proc. 14th Telecommun. Forum*, 2006, pp. 329–332.

[41] S. Mallat, "IX-an approximation tour," in *A Wavelet Tour of Signal Processing*, 2nd ed. New York, NY, USA: Academic Press, 1999, pp. 376–433.

[42] S. Feizi, G. Angelopoulos, V. K. Goyal, and M. Medard, "Backward adaptation for power efficient sampling," *IEEE Trans. Signal Process.*, vol. 62, no. 16, pp. 4327–4338, Aug. 2014.

[43] STMicroelectronics, "iNEMO inertial module: Always-on 3D accelerometer and 3D gyroscope," LSM6DS3 datasheet, Feb. 2016, http://www.st.com/content/ccc/resource/technical/document/datasheet/a3/f5/4f/ae/8e/44/41/d7/DM00133076.pdf/files/DM00133076.pdf/jcr:content/translations/en.DM00133076.pdf

Qi Liu received the BE degree from the Harbin Institute of Technology, China, in 2010. She is currently working toward the PhD degree in the Department of Electrical and Computer and Energy Engineering, University of Colorado, Boulder. Her current research interests include wearable computing, signal processing, and data mining. She is a student member of the IEEE.

James Williamson received the BS degree from the University of Arizona, in 2009, and the PhD degree in electrical engineering from the University of Colorado, Boulder, in 2016. His research interests include low power system design for human-borne wearable sensor systems, specifically, for applications sensing human kinematic, and human physiological information for sports, fitness, and health monitoring applications. He is a student member of the IEEE.

Kun Li received the BE degree from Xidian University, Xi'an, China, in 2006, and the PhD degree in electrical engineering from the University of Colorado, Boulder, in 2014. His current research interests include mobile computing, sensing systems, and cyber physical systems. He received the nomination for the Best Paper Award at the International Symposium on Low Power Electronics and Design in 2010 for his research.

Wyatt Mohrman received the BS degree in electrical engineering from the University of Colorado, Boulder, in 2013. His research interests include signal processing, algorithm design, and low power algorithm optimization for embedded systems. Of particular interest are biomechanics and biomedical applications using MEMS based sensors and a low power micro-controllers.

Qin Lv received the BE (Hons.) degree from Tsinghua University, Beijing, China, in 2000, and the PhD degree in computer science from Princeton University, Princeton, New Jersey, in 2006. She is an associate professor in the Department of Computer Science, University of Colorado, Boulder. Her research integrates efficient system design with effective data analysis for the management and exploration of massive data. Her research focuses on ubiquitous computing, data mining, mobile systems, social networks, and data management. Her work won the Computational Sustainability Award at Pervasive 2012, and was nominated for Best Paper Award at ISLPED 2010 and Mobiquitous 2014. Her work has more than 3,000 citations.

Robert P. Dick received the BS degree from Clarkson University, in 1996, and the PhD degree from Princeton University, in 2002. He is an associate professor in the Electrical Engineering and Computer Science Department, University of Michigan. He was a visiting professor in the Department of Electronic Engineering, Tsinghua University, in 2002, a visiting researcher with NEC Labs America, in 1999, and was on the faculty of Northwestern University from 2003-2008. He received a US National Science Foundation (NSF) CAREER award and won his department's Best Teacher of the Year Award in 2004. In 2007, his technology won a Computer world Horizon Award and his paper was selected as one of 30 in a special collection of DATE papers appearing during the past 10 years. His 2010 work won a Best Paper Award at DATE. He is an associate editor of the *IEEE Transactions on Very Large Scale Integration*, a guest editor of the *ACM Transactions on Embedded Computing Systems*, technical program committee cochair of the 2011 International Conference on Hardware/Software Codesign and System Synthesis, and serves on the technical program committees of several embedded systems and CAD/VLSI conferences. He is a member of the IEEE.

Li Shang received the BE (Hons.) degree from Tsinghua University, Beijing, China, and the PhD degree from Princeton University, Princeton, New Jersey. He is currently an associate professor in the Department of Electrical, Computer, and Energy Engineering, University of Colorado, Boulder. He served as an associate editor of the *IEEE Transactions on Very Large Scale Integration Systems* and the *ACM Journal on Emerging Technologies in Computing Systems*. He received the Best Paper Award at IEEE/ACM DATE 2010 and IASTED PDCS 2002. His work on FPGA power modeling and analysis was selected as one of the 25 Best Papers from FPGA. His work on temperature-aware on-chip networks was selected for publication in the MICRO Top Picks 2006. His work was a recipient of the Best Paper Award nominations at ISLPED 2010, ICCAD 2008, DAC 2007, and ASP-DAC 2006. He was a recipient of the Provost's Faculty Achievement Award in 2010 and his department's Best Teaching Award in 2006. He was a recipient of the NSF CAREER award. He is a member of the IEEE.

▷ **For more information on this or any other computing topic, please visit our Digital Library at** www.computer.org/publications/dlib.